

Introduction to Synthetic Aperture Radar (SAR)

Dr. Patrick Berens

Research Institute for High-Frequency Physics and Radar Techniques (FHR)
Research Establishment for Applied Science (FGAN)
53343 Wachtberg
GERMANY

berens@fgan.de

ABSTRACT

The synthetic aperture radar principle has been discovered in the early 50th. Since then, a rapid development took place all over the world and a couple of air- and space-borne systems are operational today. Progress made in technology and digital signal processing lead to very flexible systems useful for military and civilian applications.

Radar has proved to be valuable before, because of its day-and-night capability and the possibility to penetrate clouds and rain. Optical instruments however had great advantages in the interpretation of depicted objects. The great wavelength of radar signals limits the achievable resolution in cross range direction of real aperture radar systems. Thus, imaging cannot be realized using static radar systems¹. The idea of SAR was to transmit pulses and store the scene echoes along a synthetic aperture (i.e. the path of the SAR sensor) and to combine the echoes afterwards by the application of an appropriate focussing algorithm. The combination is carried out coherently.

As we will see, it is quit easy to understand the basic idea of SAR. We will show also the hardware concept or a SAR system and give an idea for a processing algorithm.

1.0 GENERAL FACTS ABOUT SAR

Today, synthetic aperture radar (SAR) plays an important role in military ground surveillance and earth observation. Since the late eighties a couple of SAR-systems have been developed for both space and airborne operation. The underlying radar principle offers advantages compared to competing sensors in infrared or visible spectral area.

This chapter describes the field of applications where SAR can be used to gain valuable information. Physical conditions like propagation of electromagnetic waves and scene reflectivity affect the choice of several radar design parameters.

1.1 Applications

SAR has got a broad range of applications. For remote sensing a couple of earth observing satellites are currently in operation, having imaging sensors working in different spectral areas. The utilisability of optical sensors depends not only on daylight but also on the actual weather conditions. Clouds and strong

¹ Later on, we will see that high resolution radar imaging requires a relative motion between the sensor and the object/scene to be imaged. It is not relevant, whether this relative motion results from scene or object motion.

rain are impenetrable for this wavelength. Infrared sensors which are applicable day and night are even more sensitive on weather conditions. Consequently, radar sensors represent a completion of the sensor collection for remote sensing. Beyond the overall availability of SAR images there are further pros for the utilization of radar. The coherent nature of SAR enables the user to process images of subsequent overflights for interferometrical analyses. Depending on the radar wavelength the radar signal will be reflected by vegetation or the ground structure. With the choice of a concrete centre frequency of the SAR sensor, the developer decides about the appearance of the resulting radar images. Different combinations of the transmit and receive polarization can also be used for instance to classify the kind of vegetation.

Also in military context, the availability of SAR is its convincing advantage. Applications in this area are wide spread: global reconnaissance is done mainly by satellite systems, aircrafts and high flying unmanned platforms carry sensors for wide area observation and miniaturized SAR equipment is used for integration into drones for battlefield surveillance. The resolution of SAR systems, which indicates the minimal distance of two small targets in the scene which can be separated in the SAR image, has been improved over the last decades up to the order of a decimetre. Advanced classification algorithms are able to identify military objects in the scene which is of great interest.

The exploitation of the relative motion between the sensor and the scene is an essential drawback of the SAR principle. While this motion can be derived completely for a fixed scene from the motion data of the SAR platform, moving objects own an additional motion component which disturbs the imaging process. For future systems an inverse SAR mode (ISAR) will be added to image moving objects. No doubt, this is an essential feature for military application. In a realistic scenario, one sensor will perform the compound task to monitor a ground area, indicate and track moving objects and finally produce highly resolved images of the moving objects for target classification.

Operation of a bi- or multi-static configuration offers some more advantages. The receiver system, including expensive acquisition electronics, need not to transmit any energy and thus can be designed hardly detectable. Stealth targets feature a minimized mono-static radar cross section (RCS). Target echoes might be considerably higher in a bi-static configuration so the probability of detection will be increased.

To close this discussion one related application should be mentioned. Ground based imaging of satellites can be done using the ISAR principle. Optical sensors are inappropriate for this task because of the great distance. However, the satellite motion can be estimated and radar images with high resolution can be obtained. This is used for damage assessment and space surveillance.

1.2 Circumstances

It has been mentioned that the propagation and reflection of electromagnetic waves strongly depends on its frequency. Figure 1 shows the atmospheric transmission for a wide frequency interval. SAR systems for wide area surveillance have to operate in frequency areas with minimal attenuation. Beyond the K_a-band only short range systems are realizable. Advantages of systems with a higher frequency are a reduced system size and a simplified processing. X-, C- and L-band are very common for airborne and spaceborne sensors.

The wavelength of transmitted signals plays an important role also for the reflection characteristics. A rough surface has completely different reflection behaviour compared to a smooth one. However, smoothness is a property which depends on the relation of the surface structure size to the wavelength. Another feature of low frequency waves is that foliage can be penetrated thus low frequency systems are useful in some situations.

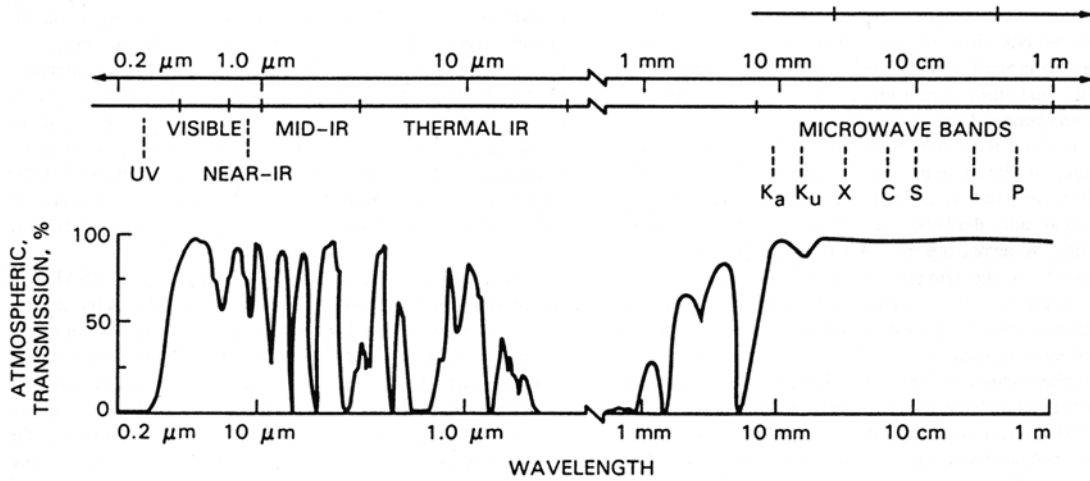


Figure 1: Atmospheric Transmission of Electromagnetic Waves in Spectral Areas of Visible Light and Different Radar Bands. (NASA 1989)

1.3 Systems and Development

Over the years a couple of systems have been built and operated by different nations. Table 1 shows some systems to give an impression of the variety.

Table 1: Some Orbital and Airborne SAR Systems Showing the Variety of Imaging Radar Systems

Shuttle missions	SIR-A	1981	40 m × 40 m	L
	SIR-B	1984	25 m × 17 m	L
	SIR-C	1994	10 m × 30 m	L, C, X
	X-SAR/SRTM	2000	25 m × 25 m	C, X
Satellite based	Lacrosse	1988	< 1 m × 1 m	X
	ERS-1	1991	26 m × 28 m	C
	J-ERS-1	1992	18 m × 18 m	L
	RADARSAT	1995	10 m × 9 m	C
	ENVISAT	2002	25 m × 25 m	C
	TerraSAR-X	2006	< 1 m × 1 m	X
	Radarsat II	2005	3 m × 3 m	C
	SAR-Lupe	2005	< 1 m × 1 m	X
Airborne SAR	IGS-2b	2008	30 cm × 30 cm	X
	DOSAR	1989	< 1 m × 1 m	S,C,X,Ka
	CARABAS-II	1997	3 m × 3 m	VHF
	PAMIR	2003	10 cm × 10 cm	X
	Lynx	1999	10 cm × 10 cm	Ku
	MISAR	2003	0.5 m × 0.5 m	Ka
	RAMSES	1994	10 cm × 10 cm	P,L,S,C,X,Ku,Ka,W
MEMPHIS	1997	20 cm × 20 cm	Ka,W	
E-SAR	1994	1.5 m × 1.5 m	P,L,S,C,X	

2.0 SYNTHETIC APERTURE RADAR

2.1 Principle

This section shows some basics of the SAR principle. The presentation comprises the fundamental facts which will be declared by descriptive considerations. Mathematical details are avoided for the benefit of understanding.

Assume a planar formation as depicted in Figure 2 a), given in the coordinates x and y . A radar sensor at a known location on the x -axis transmits a short pulse² and receives the echoes reflected by an object of the scene. The SAR-system stores the received signals in a two-dimensional data array which is parameterised in radar position and echo signal delay which is denoted by t in the figure. The proportional relation of the delay t and the object distance r allows the use of the distance parameter r instead of the parameter t . According to the distance of all scene elements the echoes superpose each other and result in the recorded data column. The data column contains a range profile.

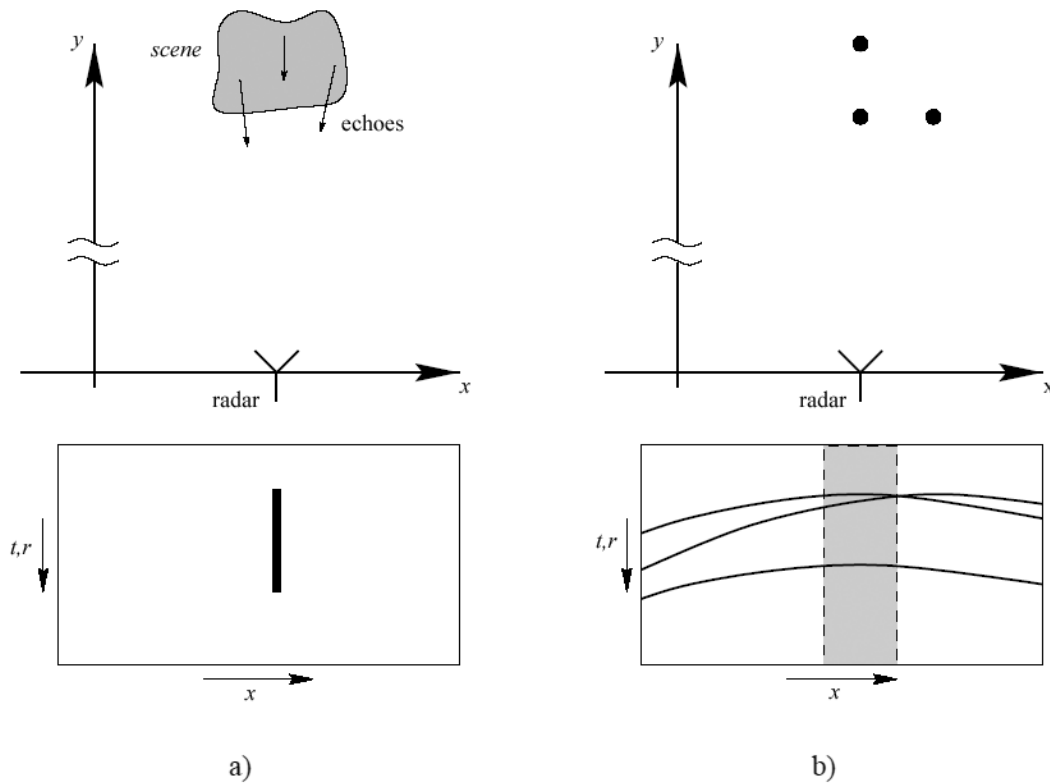


Figure 2: Two-Dimensional SAR Geometry: a) data column of a distributed scene for a fixed antenna, b) data of point targets for a moving antenna.

Below, we consider a simplified scene as depicted in Figure 2 b). Three point targets³ are given at different positions. The antenna moves in the direction of the x -axis. Since the velocity of the radar signals is very large compared to the sensor velocity, the geometry can be assumed to be static for one transmit-receive-cycle. Quasi, the antenna moves steplike. A hyperbolic range history in the data array results for each

² Real systems use extended pulses which will be compressed in the processing chain. For clarity we disregard this fact here.

³ A point target is a small object with a reflectivity which can be assumed to be at one discrete position. Corner reflectors are often used as point targets.

reflector like it is indicated by the curves in Figure 2 b). Points will be generated in a second data array at the positions of the hyperbola vertex. If the signal intensity of the individual echoes which results from the reflectivity of the scene points controls the brightness of the points in the second data array, an image of the scene results. For a realistic scene one can imagine, that it is composed of innumerable point targets. Optimized algorithms for image generation focus the distributed energy of the raw data for all scene locations simultaneously.

Now, we will discuss the achievable resolution which denotes the maximal distance of two identical point targets which can be separated in the SAR image. Since slant range resolution (resolution in y -direction) and the resolution in flight direction (x -direction) depend on different facts we discuss them one after the other.

Using short unmodulated pulses like in this contribution leads to a range resolution which is proportional to the pulse duration. In the case of rectangular pulses the pulse duration is reciprocal the signal bandwidth. A precise analysis shows that the essential criterion for the achievable resolution is not the duration but the bandwidth of the processed signal if the possibility of pulse compression is exploited. Today, radar systems commonly use long pulses with large bandwidth because they offer high resolution on one hand and a convenient power ratio.

The distance which has been covered by a reflected radar signal can be determined very precise except for a multiple of its wavelength. Thus, the range changes caused by changes of the geometry can be measured using periodical pulse repetition. The accuracy of this measurement is better the smaller the signal wavelength is. The thickness of the hyperbolas in Figure 2 b) can be chosen proportional to the wavelength to illustrate the influence of the measurement accuracy. If we analyse the hyperbolic range histories of two point targets slightly shifted in x -direction, two factors can be identified which affect the separability of the hyperbolas. If the lines become too thick, the hyperbolas merge and cannot be divided. On the other hand, limitations of the data array in flight direction as is depicted in Figure 2 b) by the dashed box, cause a reduced separability of the targets. A mathematical analysis confirms these thoughts with the result that the resolution in flight direction is approximately proportional to the quotient of the wavelength and the aspect angle interval from which the radar signals are reflected by the scene. Two consequences should be mentioned: Since the observation angle cannot be arbitrarily increased, the resolution in flight direction is limited⁴. Operating a SAR system in the common stripmap mode with a fixed antenna look-direction relating to the flight direction, the antenna beam pattern determines the observation angle (equals the angle of beam). A range independent resolution results. The observation time of an individual scene scatterer (reflecting element) increases proportional to the distance.

Now we extend the presentation to a three-dimensional geometry to check what happens in the case of imaging a special scene reflectivity. Scatterers of the scene which will be passed by the SAR sensor at the same time in the same distance feature identical range histories and therefore superpose in one image pixel. The interpretation of SAR images has to account for this effect.

The design of modern SAR systems demands for increasing resolution capabilities. The limitation which is induced by the operation in stripmap mode has become a problem. By using a small antenna the angle of beam and so the observation angle might be increased. Thereby, the antenna gain would decrease and the operational range recedes. Moreover, a short antenna demands for short distances between subsequent pulses which also leads to range limitations. Thus, the realisation of long range systems is impossible using this operational mode. The operation in spotlight mode solves this problem: While the sensor platform passes the scene, the antenna beam will be steered so that the scene will be illuminated over a large aspect angle. By this means both demands can be satisfied: The operation of a high gain antenna and

⁴ The theoretical resolution which can be reached observing the scene over 180° aspect angle is a quarter of the wavelength.

the observation over a large aspect angle. Consequently most SAR systems currently under development incorporate the spotlight mode.

2.2 Imaging in Range Direction

As mentioned before, modern radar systems transmit broadband signals and compress the received echoes. This section describes imaging in one direction, concrete in range direction and incorporates pulse compression. Also, the presentation introduces the notation in spatial and wavenumber domain which turned out to be practical.

An antenna transmits the signal $\tilde{s}_t(t)$ which will be reflected by a point target with reflectivity α having a distance r' from the sensor. The signal propagates with velocity c . The received signal $\tilde{Z}(t)$ is composed of the echo $\tilde{s}_r(t) = \alpha\tilde{s}_t(t - \tau)$ and thermal noise $\tilde{N}(t)$. Here, $\tau = 2r'/c$ is the signal propagation time.

$$\tilde{Z}(t) = \tilde{s}_r(t) + \tilde{N}(t)$$

This simple model neglects for propagation losses. A filter with impulse response $\tilde{h}(t)$ compresses the received signal. A criterion for the efficiency of the combination of the transmit signal and the compression filter is the output of the filter if the transmit signal is compressed. This results in the point target response (also known as point spread function)

$$\tilde{p}(t) = (\tilde{h} * \tilde{s}_t)(t).$$

The asterisk is used as the convolution operator. Several aspects have an influence on the choice of the compression filter function. The optimisation of the signal-to-noise ratio for $t = \tau$ is presented in [11]. The result is the matched filter which has the impulse response $\tilde{h}_m(t) = \tilde{s}_t(-t)$. In this case, the point target response becomes the autocorrelation function

$$\tilde{p}_m(t) = \int_{-\infty}^{\infty} \tilde{s}_t(t')\tilde{s}_t(t + t')dt'$$

of the transmit signal. If $\dot{\tilde{s}}_t(\omega)$, $\dot{\tilde{p}}(\omega)$ and $\dot{\tilde{h}}(\omega)$ denote the transmit signal, the point spread function and the transfer function of the compression filter, respectively, the filter function can be expressed as

$$\dot{\tilde{p}}(\omega) = \dot{\tilde{h}}(\omega) \dot{\tilde{s}}_t(\omega).$$

The bullet over the signal symbol denotes that the function is given in frequency domain. In the case of matched filtering we get

$$\dot{\tilde{p}}_m(\omega) = \dot{\tilde{s}}_t(\omega)^* \dot{\tilde{s}}_t(\omega) = \left| \dot{\tilde{s}}_t(\omega) \right|^2, \quad \text{where} \quad \dot{\tilde{h}}_m(\omega) = \dot{\tilde{s}}_t(\omega)^*$$

The asterisk denotes the conjugate operator. Thus, the spectrum of the transmit signal determines the point spread function.

Now, we alter the presentation to spatial and wave number domain. Mathematical expressions will become more compact and clear. According to the time signals $\tilde{s}_t(t)$ and $\tilde{h}(t)$ we define

$$s_t(r) = \tilde{s}_t(2r/c) \quad \text{and} \quad h(r) = \tilde{h}(2r/c)$$

and the point spread function $p(r) = (h * s_t)(r) = c\tilde{p}(2r/c)/2$.

Usually, the wave number \bar{k}_r of a signal, having the wavelength λ is determined by $2\pi/\lambda$. However, in the radar case two-way propagation has to be taken into account, so an equivalent wavelength $k_r = 4\pi/\lambda$ will be used. In this case, transformation relations are expressed by

$$\dot{s}(k_r) = \int_{-\infty}^{\infty} s(r)e^{-jk_r r} dr \quad \text{and}$$

$$s(r) = \frac{1}{2\pi} \int_{-\infty}^{\infty} \dot{s}(k_r)e^{jk_r r} dk_r$$

The point spread function in the case of matched filtering becomes

$$p_m(r) = \frac{1}{2\pi} \int_{-\infty}^{\infty} |\dot{s}_t(k_r)|^2 e^{jk_r r} dk_r.$$

Obviously, the spectral power density $|\dot{s}_t(k_r)|^2$ results in a weighting in the wave number domain. The range imaging problem of a point target in distance r' without noise leads to the received signal $z(r) = \alpha s_t(r - r')$. The output signal

$$z_h(r) = (h * z)(r) = \alpha p(r - r')$$

of the system for an arbitrary compression filter $h(r)$. This is a scaled and shifted version of the point spread function. Finally, we can extend the presentation to a continuous reflectivity distribution. A reflectivity $a(t)$ returns echoes of the transmit signal $s_t(r)$ which superpose to the signal

$$z(r) = \int_{-\infty}^{\infty} a(r')s_t(r - r')dr' = (a * s_t)(r)$$

Application of a compression filter with impulse response $h(r)$ leads to

$$z_h(r) = (h * z)(r) = (h * a * s_t)(r) = (p * a)(r).$$

The filtered receive signal $z_h(r)$ also known as range profile results as the convolution of the scene reflectivity and the point spread function. In the wave number domain this expression is a simple multiplication of the two signals.

2.3 SAR Data Model

SAR exploits the sensor motion to span a large aperture to reach a resolution which is much finer than the resolution of the real antenna. The data acquisition takes place in two directions. The first direction is range which was discussed in the previous section. Repetition of the cycle ‘transmit pulse – receive echoes’ during the sensor motion constitutes the second dimension. Different parameters are authoritative for both directions: While the velocity of light plays an important role in range direction, the sensor motion is important in flight direction. Because of these relations, slow and fast-time are well known terms for the time parameters in flight and range direction, respectively. Following on, we develop a signal model, incorporating the sensor motion.

2.3.1 General Model

The sensor platform moves along a path which is described by the vector \underline{b} . Along this path, an antenna transmits pulses and receives the echoes of a scene. We suppose, that the platform retains its position during signal propagation. Thus, the Doppler-effect can be neglected for single pulses. The vector \underline{p} denotes a position of the scene, where an echo will be reflected.

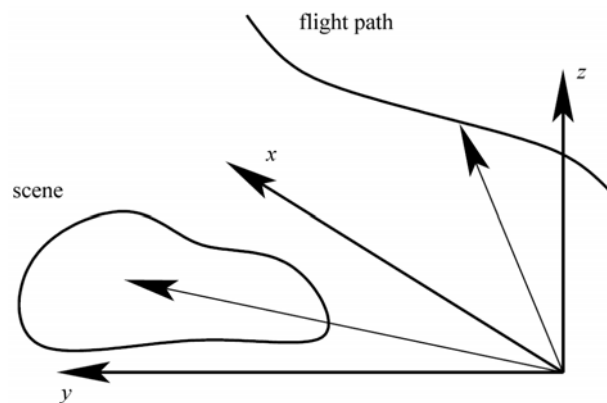


Figure 3: Geometry for General Model.

The signal model contains several terms:

- The amplitude of the propagated electromagnetic wave decreases inverse proportional to the distance. After the reflection, this effect happens in an equal way, thus it has to be incorporated in the received signal quadratically.
- The antenna of a SAR system has to account for a couple of different criterions. Such an antenna has an antenna beam which leads to an individual illumination. This illumination of the scene can be described by the function $g_a(\underline{p}; \underline{b})$, where \underline{b} is a position of the sensor path. The fact, that the antenna characteristics influence the signal twice has been taken into account in the choice of g_a .
- Equivalent to the one-dimensional presentation, the reflectivity $a(\underline{p})$ denotes the ability of the scene to reflect an incident signal. The aim of the data processing is to extract information about this reflectivity from the recorded raw data. The depiction of the reflectivity is the SAR image of the scene.
- The transmit signal will be shifted according to the distance of the radar sensor at the current position and the target location.

All partial echoes superpose to the scene echo

$$s_a(\underline{b}, r) = \iiint_{\underline{p}} \frac{g_a(\underline{p}; \underline{b})}{d_a^2(\underline{p}, \underline{b})} a(\underline{p}) s_t(r - d_a(\underline{p}, \underline{b})) d\underline{p},$$

where $d_a(\underline{p}, \underline{b}) = |\underline{p} - \underline{b}|$ is the distance of the two positions. The index a marks the general model. In flight direction, the sampling results from the repetition of the transmit receive procedure.

2.3.2 Model for a Straight Line

Most algorithms for SAR processing presume a straight flight path. Deviations will be handled as motion errors. However, there exist also historical reasons for the constraint of the straight flight: The idea of SAR was to virtually create a large aperture comparable to a linear array antenna.

Given a base location \underline{b}_0 , a directional vector \underline{b}_d and a path parameter κ , a straight flight path can be described by

$$\underline{b}(\kappa) = \underline{b}_0 + \kappa \underline{b}_d.$$

The sensor approaches a point \underline{p} of the scene at path position $\underline{b}(\kappa_\perp)$ if

$$\kappa_\perp = \frac{(\underline{p} - \underline{b}_0)^T \underline{b}_d}{|\underline{b}_d|^2} \quad \text{with} \quad |\underline{b}_d|^2 = \underline{b}_d^T \underline{b}_d.$$

At this position, the scene point lays exactly broadside the sensor. The distance between the sensor and the scene point can be calculated for other path positions by

$$\begin{aligned} d_a(\underline{p}, \underline{b}(\kappa)) &= |\underline{p} - \underline{b}(\kappa)| = |(\underline{p} - \underline{b}_0) - (\kappa - \kappa_\perp) \underline{b}_d| \\ &= d_a(\underline{p}, \underline{b}_0) \sqrt{1 + (\kappa - \kappa_\perp)^2 \frac{|\underline{b}_d|^2}{d_a^2(\underline{p}, \underline{b}_0)}}. \end{aligned}$$

As mentioned before, the result is a hyperbolic range history. For the special case of a motion in x -direction, a base location with zero y -component, a normalized direction vector as well as $\underline{p} = (p_x; p_y; p_z)^T$, $\underline{b} = (b_x; 0; b_z)^T$ and $\underline{b}_0 = (b_{0,x}; 0; b_{0,z})^T$, some relations follow:

$$\kappa_\perp = p_x - b_{0,x},$$

$$d(\underline{p}, b_x) = d_a(\underline{p}, \underline{b}) = p_\rho \sqrt{1 + \frac{(b_x - p_x)^2}{p_\rho^2}} \quad \text{and}$$

$$p_\rho = d_a(\underline{p}, \underline{b}_\perp) = \sqrt{p_y^2 + (p_z - b_{0,z})^2}.$$

The illumination function $g(\underline{p}; b_x)$ results from g_a by evaluation along the straight path. The index g denotes the model for the straight flight.

2.3.3 Imaging of a Point Target

The presentation can be reduced to point targets since the received signal is a superposition of their echoes. Insight can be transferred to complex scenes if signal processing is also linear. The scene might consist of one point at position $\underline{p}_0 = (p_{0,x}, p_{0,y}, p_{0,z})$ with reflectivity $a_0(\underline{p}) = \alpha \delta(\underline{p} - \underline{p}_0)$. The function $\delta(\underline{r})$ is the Dirac delta. The echo of the scene becomes

$$s_g(b_x, r) = \iiint_{\underline{p}} \frac{g(\underline{p}; b_x)}{d^2(\underline{p}, b_x)} a(\underline{p}) s_t(r - d(\underline{p}, b_x)) d\underline{p}$$

A two-dimensional compression can be realized by applying a two-dimensional matched filter which can be derived from the reference function. The reference function can be derived from the expected result of a point target at the location \underline{q} having the same coordinates in y - and z -direction, but at zero x -position. If g is invariant according to translation in x -direction, the reference function

$$\begin{aligned} s_{ref}(b_x, r) &= \frac{g(\underline{q}; b_x)}{d^2(\underline{q}, b_x)} s_t(r - d(\underline{q}, b_x)) \\ &= \frac{g(\underline{p}_0; b_x + p_{0,x})}{d^2(\underline{p}_0, b_x + p_{0,x})} s_t(r - d(\underline{p}_0, b_x + p_{0,x})) \end{aligned}$$

results. In the two-dimensional wave number domain, the matched filtering can be written as

$$\ddot{z}_m(k_x, k_r) = \ddot{s}(k_x, k_r) \ddot{s}_{ref}(k_x, k_r)^* = \alpha |\ddot{s}_{ref}(k_x, k_r)|^2 e^{-jk_x p_{0,x}}$$

The two closed bullets above the signal letters denote that both parameters of the functions are given in wave number domain. Later we will also work with functions having one spatial and one wave number domain argument. In addition, we will then use a bullet and a circle instead. The image of the point target results after an inverse Fourier transform:

$$z_m(x, r) = \alpha p_m(x - p_{0,x}, r), \quad \text{with} \quad p_m(x, r) = \mathcal{F}_2^{-1} \left\{ |\ddot{s}_{ref}(k_x, k_r)|^2 \right\}$$

The absolute value of the two-dimensional point spread function $p_m(x, r)$ has a maximum at the origin which grows with the covered area of the reference function in wave number domain. The image of the considered point target thus appears at position $(p_{0,x}, 0)$ which reproduces the correct location in x -direction. Position 0 in range direction means here, that the imaged point has the same distance than the reference point which was assumed to produce the reference function. The resolution which can be achieved in flight direction depends on the covered wave number domain area in k_x . We introduce $K_x = \max(k_x) - \min(k_x)$, the length of the covered interval. The signal phase of the reference function for a mono-frequent transmit signal

$$s_{ref}(b_x, r) = \frac{g(\underline{p}_0; b_x + p_{0,x})}{d^2(\underline{p}_0, b_x + p_{0,x})} e^{jk_r, 0(r - d(\underline{p}_0, b_x + p_{0,x}))}$$

can be used to determine the wave number

$$k_x(b_x) = \frac{\partial}{\partial b_x} k_{r,0}(r - d(\underline{p}_0, b_x + p_{0,x})) = -k_{r,0} \frac{b_x}{\sqrt{p_{0,\rho}^2 + b_x^2}},$$

where $p_{0,\rho}$ is the distance of the analysed point to the flight path. The antenna characteristic can be approximated by a rectangular function. If we denote the angle between the flight direction and the direction to the point target by φ and its cosine by u , this characteristic can be written by $|u| = |\cos(\varphi)| \leq u_g$. The illumination function $g(\underline{p}_0; b_x + p_{0,x})$ thus can be converted to

$$|b_x| \leq u_g \sqrt{p_{0,\rho}^2 + b_x^2}$$

and

$$-\frac{K_x}{2} = -k_{r,0} u_g \leq k_x(b_x) \leq k_{r,0} u_g = \frac{K_x}{2}$$

limits the ‘visible’ area in wave number domain. This rectangular weighting in wave number domain leads to an si-function in spatial domain, after the inverse Fourier transform. The Rayleigh resolution is $\delta_x = \pi / (k_{r,0} u_g) = 2\pi / K_x$. Obviously, the resolution is independent of the point target distance. The assumptions made here represent the operation in stripmap mode.

2.3.4 Signal Model in Wave Number Domain

We have shown that the covered area in wave number domain plays an important role for the imaging capability of a SAR system. Moreover, the last section demonstrated that the compression can be realized efficiently in the wave number domain using simple multiplications. This fact motivates to analyse the data in the two-dimensional wave number domain. The Fourier transformation

$$\ddot{s}(k_x, k_r) = \int_{-\infty}^{\infty} \int_{-\infty}^{\infty} s(b_x, r) e^{-j(k_r r + k_x b_x)} dr db_x$$

of the echo of a point target can be determined analytically. The Fourier transformation in range direction leads to

$$\begin{aligned} \dot{s}(b_x, k_r) &= \int_{-\infty}^{\infty} s(b_x, r) e^{-jk_r r} dr \\ &= \alpha \frac{g(\underline{p}_0; b_x)}{d^2(\underline{p}_0, b_x)} \dot{s}_t(k_r) e^{-jk_r d(\underline{p}_0, b_x)} \end{aligned}$$

The next step converts the signal in wave number domain also in the direction of x . We evaluate

$$\ddot{s}(k_x, k_r) = \int_{-\infty}^{\infty} \dot{s}(b_x, k_r) e^{-jk_x b_x} db_x$$

An exact expression cannot be determined. However, the principle of stationary phase (see [2] for information about the principle of stationary phase) enables us to approximate the integral. The idea is to

find one stationary point \bar{b}_x which particularly governs the value of the integral. Other positions did not contribute noticeable because of fast fluctuations of the phase term. The b_x -dependant phase term of the integrand is

$$\Phi(\underline{p}_0, b_x) = -k_r d(\underline{p}_0, b_x) - k_x b_x$$

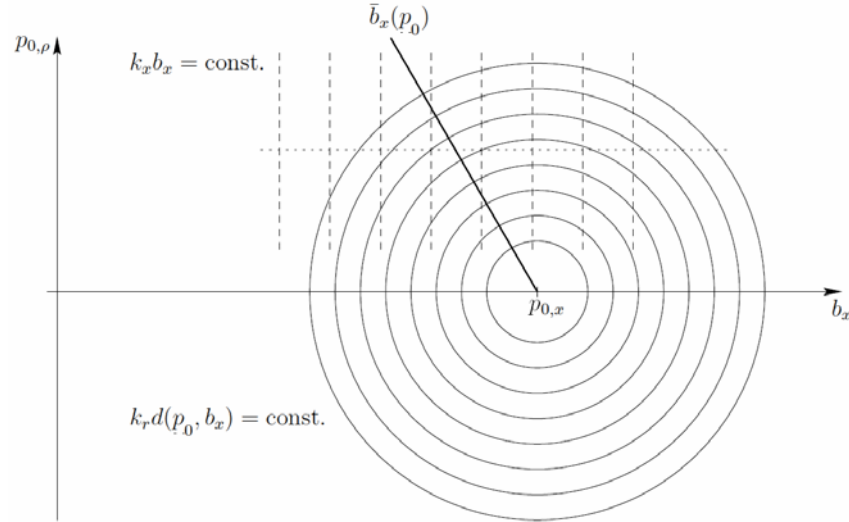


Figure 4: Illustration of Phase Terms to Interpret the Principle of Stationary Phase.

Figure 4 depicts the addends of the phase. If k_r is chosen, the contour lines of $k_r d(\underline{p}_0, b_x)$ are circles in the depicted plane. The contour lines of $k_x b_x$ are dashed lines in the figure. The dotted line marks the path of integration for one concrete $p_{0,\rho}$. Along this line we find the stationary point where the contour lines possess the same distance in x -direction. Stationary points fulfil the condition

$$0 = \left. \frac{d\Phi(b_x)}{db_x} \right|_{\bar{b}_x(\underline{p}_0)} = -k_r \frac{\bar{b}_x(\underline{p}_0) - p_{0,x}}{\sqrt{p_{0,\rho}^2 + (\bar{b}_x(\underline{p}_0) - p_{0,x})^2}} - k_x$$

and we find after some steps one stationary point for

$$\bar{b}_x(\underline{p}_0) = p_{0,x} - \frac{k_x}{\sqrt{k_r^2 - k_x^2}} p_{0,\rho}$$

The line in Figure 4 depicts the locations of stationary points for a fixed $p_{0,x}$ and variable $p_{0,\rho}$. The stationary phase for this point results in

$$\begin{aligned} \Phi(\bar{b}_x) &= -k_r d(\underline{p}_0, \bar{b}_x(\underline{p}_0)) - k_x \bar{b}_x(\underline{p}_0) \\ &= \frac{k_r^2}{k_x} (\bar{b}_x(\underline{p}_0) - p_{0,x}) - k_x \bar{b}_x(\underline{p}_0) \\ &= \frac{k_r^2 - k_x^2}{k_x} (\bar{b}_x(\underline{p}_0) - p_{0,x}) - k_x p_{0,x} \\ &= -\sqrt{k_r^2 - k_x^2} p_{0,\rho} - k_x p_{0,x}, \end{aligned}$$

Thus, we get the following wave number domain model for the echo signal of a point target:

$$\ddot{s}(k_x, k_r) = \alpha w_1 \dot{s}_t(k_r) \frac{g\left(\underline{p}_0; p_{0,x} - \frac{k_x}{\sqrt{k_r^2 - k_x^2}} p_{0,\rho}\right)}{d^2\left(\underline{q}, -\frac{k_x}{\sqrt{k_r^2 - k_x^2}} p_{0,\rho}\right)} e^{-j\sqrt{k_r^2 - k_x^2} p_{0,\rho}} e^{-jk_x p_{0,x}}$$

The amplitude term w_1 results from the principle of stationary phase. However, this term plays a minor role in SAR processing.

2.4 SAR System

Main parts of a SAR system are depicted in Figure 5. A pulse generation unit creates pulses with a bandwidth according to the aspired range resolution. They will be amplified by the sender and are transferred to the antenna via a circulator. The receiver gets the antenna output signal (echoes of the scene) amplifies them to an appropriate level and applies a bandpass filter. After the demodulation and A/D conversion of the signals the SAR processor starts to calculate the SAR image. Additional motion information will be provided by a motion measurement system. A radar control unit arranges the operation sequence, particularly the time schedule.

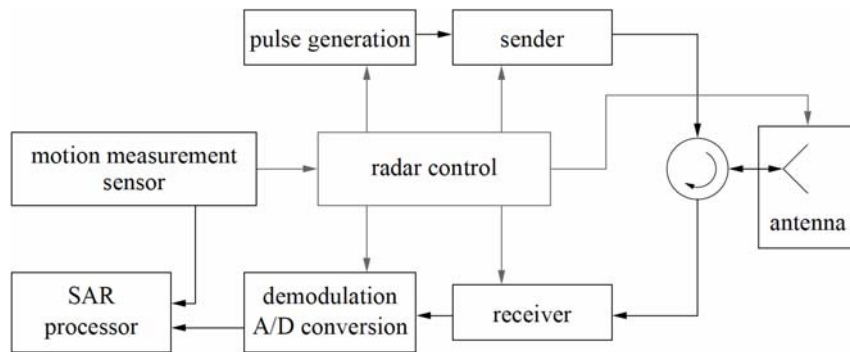


Figure 5: General Structure of a SAR System.

2.5 Processing of Radar Data

Over the years, a couple of processing algorithms have been developed. At first, separated processing approaches have been implemented, which sequentially solved the problems of range and azimuth (in flight direction) compression. These methods are well documented in the literature as range Doppler processing. With the increasing performance of newly developed systems, these processing algorithms reached their limitations which originate from implied approximations. Latest developments are useful to process data up to any resolution. However, the efficiency has to be bought by extensive hardware investment.

Following on, we will present one processing strategy. The signal model of a point target in wave number domain has been derived in section 2.3.4. Analysing the phase of that signal, we find that it is non-linear in the wave number coordinates. The idea of the range migration algorithm (also known as $\omega - k$ -algorithm) is to introduce a new coordinate in the wave number domain so that the signal gets a linear phase in the new coordinate system. The substitution

$$k_\rho = \sqrt{k_r^2 - k_x^2}$$

solves this problem. An inverse Fourier transform leads to the SAR image of the point target. (The amplitude term is the wave number representation of the point spread function and the linear phase term provides the correct location after the transformation.) Within the implementation the substitution enables a resampling in the new coordinate k_ρ . The new samples will be calculated using the so-called Stolt-interpolation.

Further information about SAR data processing can be found in a couple of books which are given in the literature list.

3.0 LITERATURE

- [1] P. Berens, *Neue Signalverarbeitungsverfahren für SAR im Scheinwerfermodus*, Shaker Verlag, Aachen, 2003.
- [2] W. G. Carrara, R. S. Goodman and R. M. Majewski, *Spotlight Synthetic Aperture Radar: Signal Processing Algorithms*, Artech House, Norwood, MA, 1995.
- [3] J. C. Curlander and R. N. McDonough, *Synthetic Aperture Radar: Systems and Signal Processing*, Wiley-Interscience:Series in Remote Sensing, New York, 1991.
- [4] M. D. Desai and W. K. Jenkins, Convolution backprojections image reconstruction for spotlight mode synthetic aperture radar, *IEEE Transactions on Image Processing*, Vol. 1, No. 4, pp. 505-517, 1992.
- [5] J. H. G. Ender, The meaning of k-space for classical and advanced SAR-techniques, in *Proc. PSIP'2001*, 2001.
- [6] F. M. Henderson, A. J. Lewis, et al, *Principles & Applications of Imaging Radar – Manual of Remote Sensing* (3rd edition, volume 2), John Wiley & Sons, New York, 1998.
- [7] H. Klausing and W. Holpp (Ed.), *Radar mit realer und synthetischer Apertur*, Oldenbourg, München, 2000.
- [8] R. Lanari and G. Fornaro, A short discussion on the exact compensation of the SAR range dependent range cell migration effect, *IEEE Trans. on Geoscience and Remote Sensing*, Vol. 35, No. 6, pp. 1446-1452, 1997.
- [9] R. K. Raney, A new and fundamental Fourier transform pair, in *Proc. IGARSS'92*, pp. 106-107, 1992.
- [10] R. K. Raney, H. Runge, R. Bamler, I. G. Cumming and F. H. Wong, Precision SAR processing using chirp scaling, *IEEE Transactions on Geoscience and Remote Sensing*, Vol. 32, No. 4, pp. 786-799, 1994.
- [11] M. I. Skolnik, *Introduction to Radar Systems*, McGraw-Hill, New York, 1980.
- [12] M. Soumekh, *Synthetic Aperture Radar Signal Processing with MATLAB Algorithms*, Wiley-Interscience, New York, 1999.
- [13] A. F. Yegulalp, Fast backprojection algorithm for synthetic aperture radar, in *The Record of the 1999 IEEE Radar Conference*, pp. 60-65, 1999.